sciendo

GEOLOGOS

Geologos 26, 3 (2020): 219–231
DOI: 10.2478/logos-2020-0021

Mineralogy and geochemistry of rare earth elements in the Moyil Valley alteration zones, Meshkinshahr (northwest Iran)

Hossain Naseri[1], Mahnaz Jamadi[1], Kaikhosrov Radmard[2]*, Ghafour Alavi[1]

[1]Department of Earth Sciences, Faculty of Natural Sciences, University of Tabriz, Tabriz, Iran
[2]Department of Geology, Faculty of Natural Sciences, Lorestan University, Khoram Abad, Iran
*corresponding author, e-mail: kaikhosrov@gmail.com

Abstract

Sabalan Mountain (northwest Iran) witnessed intense volcanic activity during the Cenozoic (Plio-Pleistocene). The result of this manifests itself in the conical geometry of the Sabalan stratovolcano and ahigh hydrothermal gradient around it, which can be detected by geological phenomena such as hot springs, smoke gases and steam outlet pores. The high hydrothermal slope and upward migration of hot water in this area have caused extensive alteration zones in the host rocks. A mineralogical study of alteration zones in thewells drilled in the Moyil Valley to the northwest of Sabalan Mountain has revealed the presence of phyllic, argillic, calcitic and propylitic alterations in volcanic rocks (trachyandesite) and alteration phyllic and propylitic ones in monzonite rocks. In chondrite-normalised rare-earth-element diagrams, trachyandesite rocks exhibit an HREEs enrichment when compared to MREEs and LREEs in propylitic and calcitic alteration zones. This result can be explained by the acidic nature of hydrothermal fluids containing complex ions such as (SO^{-2}, Cl^{-}). The $(La/Yb)_{cn}$, $(La/Sm)_{cn}$ and $(Tb/Yb)_{cn}$ ratios for argillic, phyllic, propylitic and calcitic alteration zones have revealed that they are higher in fresh rocks compared to altered rocks, suggesting the enrichment of HREEs in comparison to LREEs and MREEs. The anomalies of Eu do not change remarkably in the argillic and propylitic alteration zones of trachyandesite rocks; apparently, alteration hadno effect on them. Such behaviour reflects the presence of gold cations in Eu^{+3} formed at temperatures below 250°C. Eu anomalies increased in propylitic alteration zones in monzonite rocks and calciticand phyllic alteration zones in trachyandesiterocks.

Key words: Sabalan Mountain, Cenozoic, chondrite-normalised, HREEs, trachyandesite

1. Introduction

Volcanic activities of Mountain Sabalan, which ended in the Plio-Pleistocene, led to an increase in geothermal slope around it. Such an increase in heat gradient manifests itself in features such as hot springs, smoke and steam exits. Another consequence of the high geothermal slope is the wide expansion of alteration zones around Mount Sabalan. The present study area is located 20 km south of the city of Meshkinshahr in the province of Ardebil (northwest Iran; Fig. 1). The drilling operation started with exploration wells in November 2002, followed by three other wells in the next 18 months. The first (NWS-1), second (NWS-3) and third (NWS-4) exploration geothermal wells of Meshkinshar were drilled as deviated wells to depths of 3,197, 3,177 and 2,360 m, respectively (Fig. 2).

The most important methods used to calculate the mass changes of elements in the alteration systems are:

1. the volume factor method (Gresens, 1967; Grant, 1986);
2. the isocon method (Grant, 1986)
3. the method of low-mobility elements (Maclean & Kranidiotis, 1987; Maclean, 1990).

Although this area has been extensively studied for hydrochemistry of hydrothermal fluids in hot springs and exploratory wells, there are no studies of mineralogy and geochemistry of alteration zones in this region. In the present study, the isocon method (Grant, 1986) was used for calculation of REES and changes during development of alternation zones. For the first time, we have made an effort to combine the results of mineralogical studies, geochemical data, comprehensive information on the role of controllers, minerals and geochemical factors affecting the mobility, distribution and enrichment of rare earth elements (REEs) during alterations of rock units. It has to be noted that the occurrence of Eu and Ce anomalies can be explained by the alteration zones in the Moyil Valley.

2. Sampling and analytical methods

The present research was conducted in two phases. Field studies included exploration of the development of alteration zones and their relationship with igneous rocks and sampling of drilled cores from all three boreholes, altered zones and fresh rocks. In the laboratory study, 110 thin sections were prepared and studied at the Meshkinshahr Geothermal Workshop. In order to investigate the geochemical characteristics of the alteration zones, 22 samples (20 from altered zones and 2 from unaltered rocks) were selected for chemical analysis, using an inductively coupled plasma emission spectrometer (ICP-ES) and an inductively coupled plasma mass spectrometer (ICP-MS). The ICP-MS was sent to the ACMEAnalytical Laboratory of Canada to determine values of the main elements (Table 3 in Appendix) and partial elements including REEs (Table 4 in Appendix).

The samples from drilled exploratory wells were collected by field study to obtain the mineralogical composition of the alteration zones. X-ray fluorescence (XRF) analyses were made at Sinclair Knight Merz (SKM) laboratory under the supervision of the Renewable Energy and Energy Efficiency Organisation (Table 1).

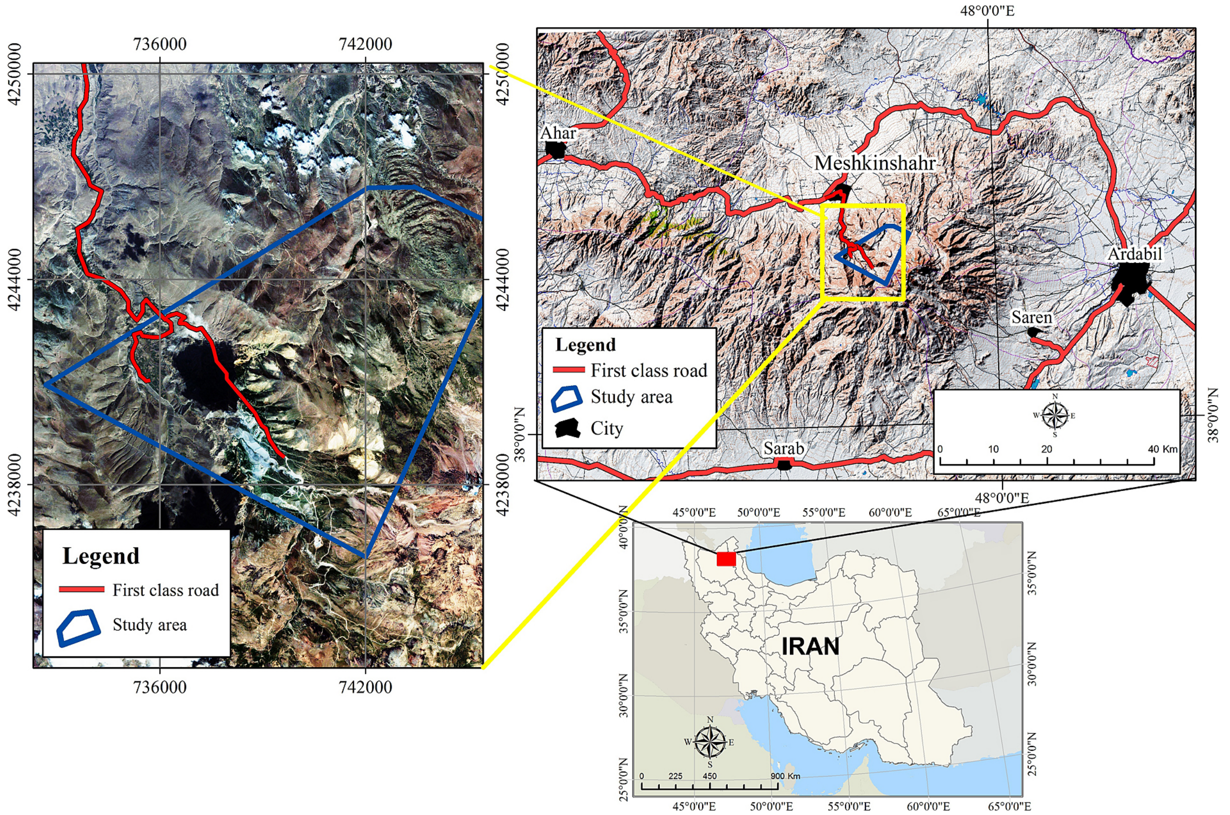

Fig. 1. Location of the Moyil Valley in northwest Iran

Table 1. X-ray diffraction (XRD) results for samples extracted from alteration zones

Sample	Alteration zone	Mineralogical composition
NWS-01-1	Argillic	Illite, smectite, kaolinite, quartz
NWS-01-2	Propylitic	Epidote, chlorite, quartz, allonite, calcite
NWS-01-3	Phyllic	Illite, chlorite, pyrite, quartz
NWS-03-1	Argillic	Illite, smectite, kaolinite, quartz
NWS-03-2	Propylitic	Epidote, chlorite, quartz, calcite
NWS-03-3	Phyllic	Illite, chlorite, pyrite, quartz
NWS-04-1	Argillic	Illite, smectite, ancerite, kaolinite, quartz
NWS-04-2	Phyllic	Illite, chlorite, pyrite, quartz, calcite

Mobility, enrichment and depletion of elements are the factors investigated by using the Grant (1986) method; it is assumed that no alterations occurred:

$$(C^A = (\rho^O / \rho^A)C^O \Delta C_i^A / C_i^O) \times 100 =$$
$$= (\rho^O / \rho^A)(C_i^A / C_i^O) - 1$$

where ρ^A, ρ^O, C_i^A, and C_i^O are the density of the altered rock, the initial rock density, the element in the altered rock and the elements in the primary rock, respectively. This method is a graphic representation of the Gresens (1967) equation. Elements that are immobile during alteration are suitable for calculating mass changes (Gresens, 1967; MacLean & Kranidiotis, 1987). In this regard, elements such as TiO_2, Al_2O_3, Zr, Hf and N, which are immobile in hydrothermal systems (Jenner, 1996; Lentz, 1996) and often have high concentrations in volcanic and non-altered plutonic rocks (Barrett & MacLean, 1994; Leitch & Lentz, 1994).

3. Geological setting

The rocks display petrographical diversity due to the formation of rock units in various volcanic phases. The study area is located in the northwest Iran region, where expansion of Cenozoic volcanic rocks is prevalent (Aghanabati, 2004) (Fig. 2).

In the study area four types of lithologies are represented (Fig. 2), as follows:

1. Valezir Formation (Pliocene): This formation is the oldest rock unit in the Sabalan volcanic complex, having formed during the Pliocene, prior to the formation of a volcanic centre. The Valehzir Formation is composed of trachyandesite, tuff and pyroclastic breccia, with a minimum thickness of 1,000 m in the region.
2. Tous Formation (early Pleistocene): The major part of this unit is composed of trachydacite, trachyandesite and rhyolite, which crop out in the form of dispersed domes and Lahar.
3. Kasra Formation (late Pleistocene): This formation is known mainly from outcrops of volcanic lava (trachyandesite), which is found mostly in the upper parts of Mountain Sabalan.
4. Dizou Formation (Quaternary): The name of this formation is taken from the village of Dizou in the Moyil Valley. The main part of this unit comprises discontinuous levels of lava of variable thickness. The most extensive development of this formation is found in the Moyil and Dizou valleys, which both overlie volcanic rocks of Pliocene age.

3.1. Lithology and stratigraphy of exploration wells

To determine the lithology and stratigraphy of the study area, cores were collected at a distance of 3 m apart from different sections of each well. Finally, 110 microscopic sections were prepared and studied under binocular and polarisation microscopes.

3.1.1. NWS-1

This is the first geothermal exploration well in the study area; it is a near-vertical borehole (Fig. 3). The youngest unit encountered is the Dizou Formation (200 m), which contains mainly conglomerates consisting of andesite and trachyandesite fragments. Between depths of 200–655 m, 655–1,021 and 1,021–3,117 m, the Valehzir Formation, the E_{pa} unit (which is highly altered and its original form is difficult to distinguish in thin sections) and the monzonite unit, respectively were documented.

3.1.2. NWS-3

This exploration well is located to the northwest of NWS-1; it was drilled down to a depth of 3,177 m (Fig. 3). The well penetrated the Dizou unit between the surface to a depth of 89 m, the Valehzir (trachyandesite and andesitic lavas) between 89 and 467 m, the Plat unit (andesite lavas, andesite, brecciated andesite, trachyandesite and lithic tuff) between 467 and 550 m, the Ngab unit (trachyandesite, trachybasalt and breccia) between 550 and 932 m, the E_{pb} unit (trachyandesite, trachybasalt, breccia and hematite tuffs) between 932 and 2,884 m, the Mejandeh metamorphic rock between 2,884 and 3,177 m, and again the E_{pb} unit between 2,781 and 3,177 (Emami, 1994).

3.1.3. NWS-4

The well was drilled to a depth of 2,260 m and penetrated the Dizou unit from the surface to a depth of 63 m, the Valezir unit between 63 and 383 m, and heavily altered early Cenozoic volcanic strata from a depth of 383 downwards to the ultimate depth reached.

4. Results and discussion

4.1. Alteration and mineralogy

The hydrothermal alteration facies were determined by mineralogical investigations, XRD and geochemical analyses. The high amount of LOI in fresh samples is due to the wide expansion of alteration zones.

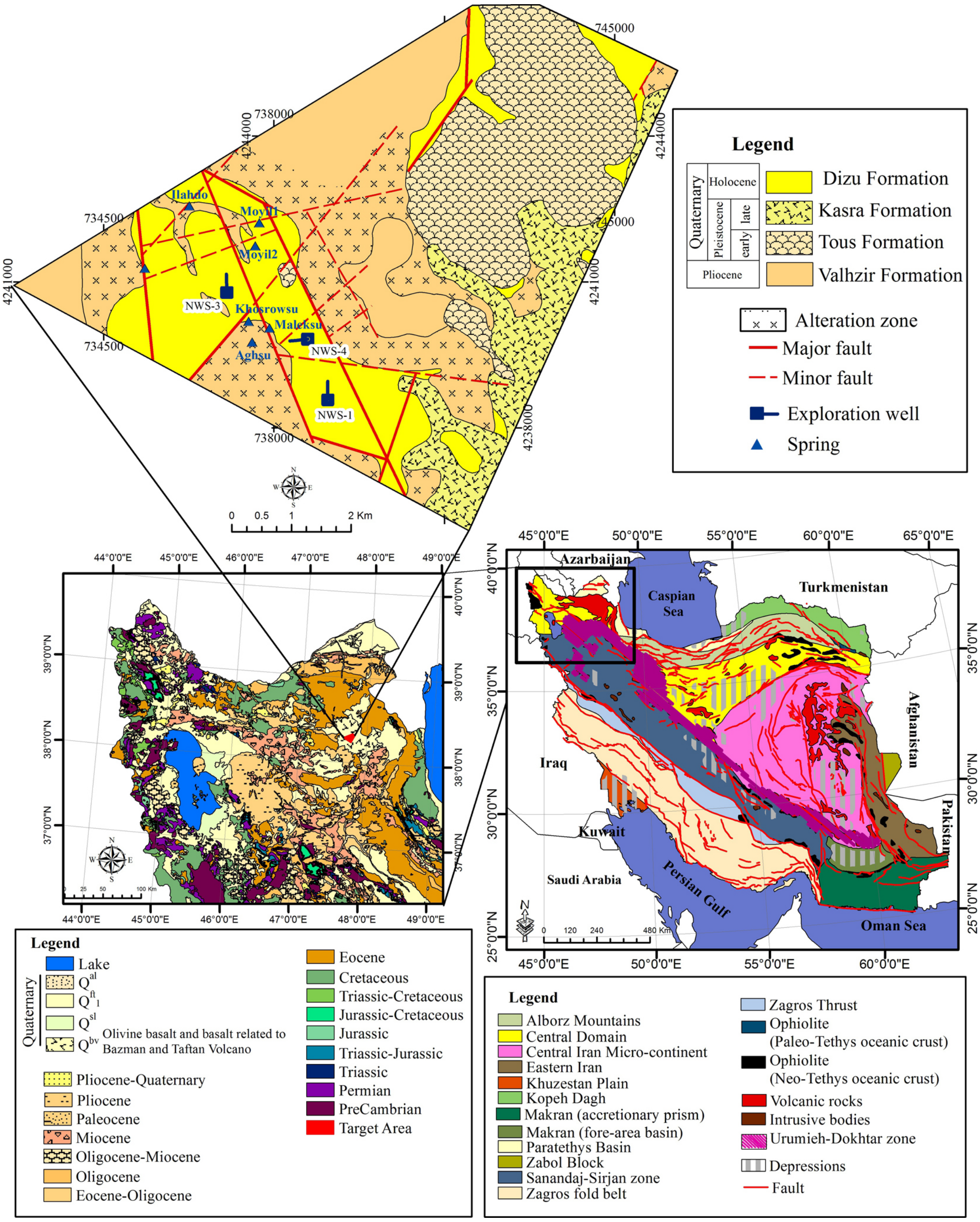

Fig. 2. Location of the study area (northwest Iran), with a simplified map of the different formations to the northwest of Mountain Sabalan (modified from Bogie et al., 2000)

In well NWS-1, four zones (i.e., non-alteration, argillic alteration zone, propylitic alteration zone and phyllic alteration zone) can be distinguished:

1. Non-alteration zone: In shallow areas (Dizou Formation) to a depth of about 200 m;
2. Argillic alteration: from a depth of about 200 to 650 m (Valehzir Formation) in wells with argillic zone mineral assemblages (i.e., illite-smectite, kaolinite and quartz);
3. Propylitic alteration: epidote, chlorite, calcite and quartz mineral assemblages in E_{pa} units and monzonite unit;
4. Phyllic alteration: sericite, chlorite, illite, quartz and pyrite mineral assemblage, which is spo-

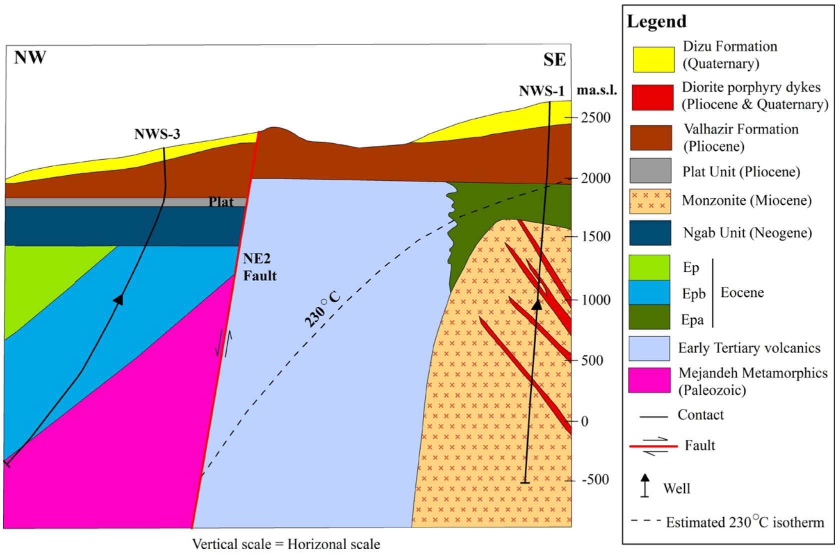

Fig. 3. Schematic transverse section of the study area and position, depth and formation of the exploration wells in the Moyil Valley

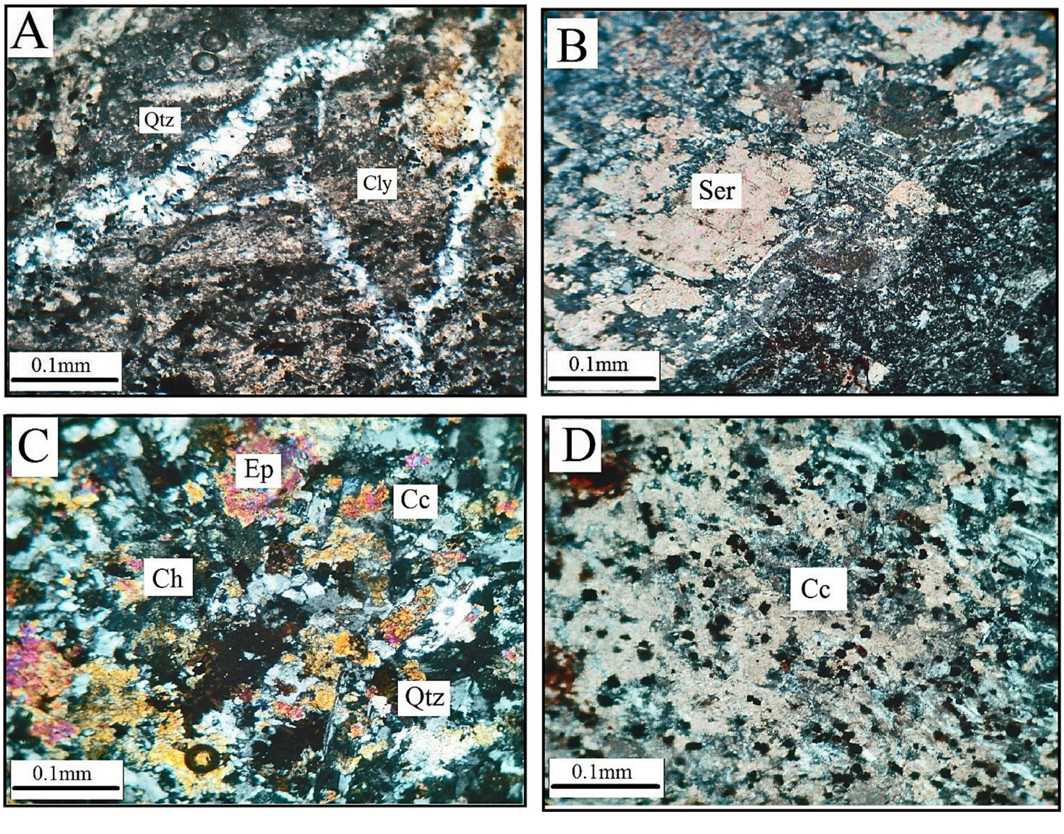

Fig. 4. Microscopic images of material from well NWS-3. **A –** Argillic alteration of clay minerals (Cly) and quartz veinlets (Qtz); **B –** Sericite (Ser) in the phyllic alteration zone; **C –**Epidote (Ep), chlorite (Ch) and calcite (Cc) in the propylitic alteration zone; **D –** Calcite (Cc) in the calcitic alteration zone

radically observed in the region of propylitic alteration.

In the NWS-3 well, hydrothermal alterations are also widely distributed; these can be divided into five zones:

1. Non-alteration zone at the surface;
2. Argillic alteration, including a rich complex of low-temperature clays such as kaolinite, smectite and illite-interlayer smectite (Fig. 4A); this mineralogical complex is composed of acid-to-neutral and low-salinity hydrothermal fluids (SKM, 2003);
3. Phyllic alteration, including illite, chlorite, quartz with pyrite and probably anhydrite alteration (Fig. 4B); this mineral assemblage formed in the presence of neutral to acidic fluids with high salinity and usually permeable zones and adjacent veins;
4. Propylitic alteration, which is characterised by the presence of chlorite, epidote, quartz, calcite and anhydrite (in very small amounts) and a small amount of illite (Fig. 4C);
5. Calcitic alteration: in some samples containing propylitic alteration, the amount of calcite is high enough to be referred to as calcitic alteration (Fig. 4D). This mineral assemblage formed in the presence of neutral pH fluids, high salinity levels and low permeability (SKM, 2003).

In the NWS-4 well, four alteration zones can be detected:

1. Non-alteration zone;
2. Argillic alteration: this complex is rich in low-temperature clay minerals, such as kaolinite and illite-interlayer smectite. This mineral assemblage consists of acidic to neutral hydrothermal fluids, with a low degree of salinity. During this alteration, clay minerals filled stone matrix and quartz filled pores;
3. Propylitic alteration: the mineral assemblage in this zone includes chlorite, epidote, quartz and calcite. This complex formed in the presence of near-neutral fluids and low salinity, and often in permeable areas;
4. Phyllic alteration: this alteration is identified by the presence of illite, sericite, quartz and pyrite. This complex formed in the presence of acidic to neutral fluids and often in areas with high permeability and a large number of veins.

4.1.1. Phyllic alteration zone

During the development of phyllic alteration, Er to Lu elements (HREEs) were enriched, while other REEs were depleted (Fig. 5A).The HREEs enrich-

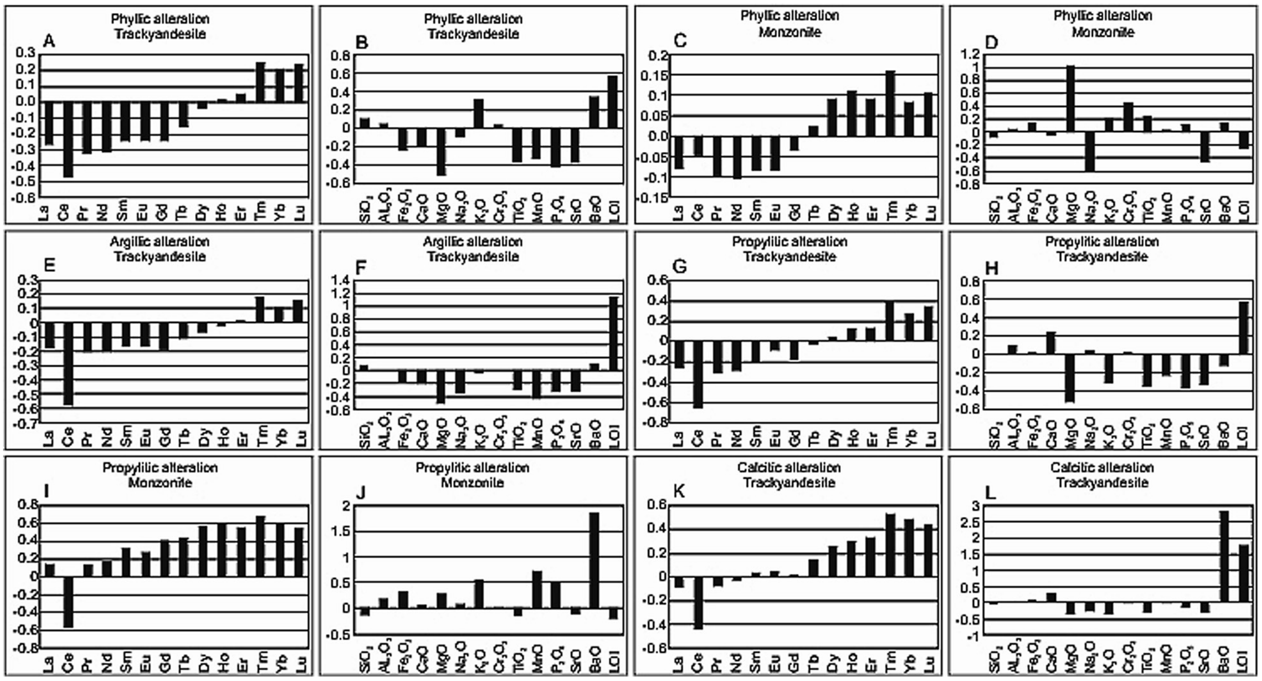

Fig. 5. Histogram corresponding to an increase or decrease in the mass of main elements and REEs hydrothermal alteration zones related to trachyandesite and monzonite rock unit. **A, B –** REEs and basic elements of the phyllic alteration zone in trachyandesite; **C, D –** REEs and main elements of the phyllic alteration zone in monzonite; **E, F –** REEs and main elements of the argillic alteration zone in trachyandesite; **G, H –** REEs and basic elements of the propylitic alteration zone in trachyandesite; **I, J –** REEs and main elements of the propylitic alteration zone in monzonite; **K, L –** REEs and main elements of the calcitic alteration zone in trachyandesite

ment in the phyllic alteration zone can be attributed to adsorption of secondary minerals that can accept REEs in their structure (Fulignati et al., 1999).

Pearson correlation coefficients are measures of the linearity or correlation between two variables. Typically, Pearson correlation coefficients greater than 0.4 are significant (dependent upon the number of samples), whereas values greater than 0.8 indicate a strong correlation between the two variables.

The high correlation coefficient of HREEs with LOI and BaO suggest the acceptance of these elements in secondary minerals such as illite and barytes (Fig. 5B). The LREEs elements have a high positive correlation (Table 5 in Appendix) with Fe_2O_3, P_2O_5, MgO and TiO_2, suggesting their adsorption by iron oxide, phosphate and titanium washed out of the system during this alteration. Typically, the separation between LREEs and HREEs during the alteration process is a function of the pH of the environment. In acidic pH, LREEs, and in alkaline pH, HREEs undergo mobility (Fulignati et al., 1999). Therefore, it can be concluded that the pH of the fluid altered acidic conditions and caused the washing out of LREEs. Accordingly, it is deduced that processes including adsorption, sweeping and acidic conditions of the fluid are the three major factors in the distribution and separation of REEs in the alteration zone. In samples 1716 and 3197 taken from the monzonite unit in well NWS-1, the LREEs and MREEs showed a similar behaviour in the phyllic alteration, while HREEs showed enrichment (Fig. 5C, D). The high correlation coefficient of HREEs with MgO in this alteration zone can be attributed to secondary magnesium minerals such as chlorite.

4.1.2. Argillic alteration zone

During the development of argillic alteration, LREE and MREE elements experienced depletion, while HREEs showed a slight relative enrichment (Fig. 5E, F). The LREE depletion suggests that acidic conditions dominated in this alteration zone and led to their leaching. The presence of illite, smectite and kaolinite minerals in the samples studied may have played an important role in HREE immobility because of their high ability to absorb and sweep REEs in alteration zones (Fulignati et al., 1999). The high correlation coefficient of LREE elements with elements such as depleted TiO_2 and P_2O_5 (Table 6 in Appendix) suggests the sweeping of REEs by their minerals. Therefore, the acidic conditions prevailing in the environment of the formation of this alteration zone, as well as the absorption of REEs, are factors that had an influence on their concentration and depletion.

4.1.3. Propylitic alteration zone

During the development of this alteration zone,the relative enrichment of HREEs compared to LREEs (Fig. 5G) may suggest the presence of low pH conditions that leached the elements of this environment. In this zone, CaO, BaO and LOI are enriched among the main oxides (Fig. 5H) and the presence of epidote and chlorite minerals can have lead to the immobility of HREEs. However, the effects of the adsorption process are not effective in the immobility of most of REEs, because the performance of adsorption processes decreases with increasing ion radius in REEs (Bau, 1991). Thus, it can be concluded that in aqueous solutions, REEs have a very strong tendency for forming complex ions (Hass et al., 1995).

In samples taken from the propylitic alteration of the monzonite unit in well NWS-1 (sample 2080), all REEs, except Ce, are enriched (Fig. 5I). In this zone, among the major oxides, Fe_2O_3, MnO and BaO show a higher enrichment compared to other oxides, probably due to the immobility of these oxides after the occurrence of alteration (Fig. 5J). REE enrichment in this zone indicates pH changes and temperature reduction, which played an important role in their mobility in alteration solutions (Michard, 1989; Lewis et al., 1997; Moore, 1998; Aubert et al., 2001). It seems that acidity of the fluid and the activity of complex ions such as SO_4^{-2}, $Cl^-$and F^- were low during the development of this alteration zone.

4.1.4. Calcitic alteration zone

During the development of the calcitic alteration, LREEs are almost depleted. MREEs have the same behaviour and all are immobile (Fig. 5K), but HREEs show enrichment (Fig. 5L). Among the main oxides in this alteration zone, BaO, LOI and CaO are enriched (Fig. 5L). The selective leaching of LREEs confirms the acidic to neutral nature of the solutions in this zone because the mobility of complex ligands such as CO_3^{-2} with HREEs is reduced by decreasing pH compared to LREEs in the solution (Lottermoser, 1990, 1992; Terkado & Fujitani, 1998; Ahmady et al., 2015).

4.2. Distribution pattern of REEs in alteration zones and elemental ratios

In order to understand the possible separation processes that REEs may undergo during alteration, the ratios $(La/Yb)_{cn}$, $(La/Sm)_{cn}$, and $(Tb/Yb)_{cn}$ were investigated for the alteration zones in the exploration wells.

4.2.1. Argillic alteration zone

The average ratios of $(La/Yb)_{cn}$, $(Tb/Yb)_{cn}$ and $(La/Sm)_{cn}$ in this alteration are 26.33, 1.93 and 5.97, respectively. These values in less altered rocks are 33.87, 2.37 and 6.6, respectively (Table 2). As shown in Figure 6A, the ratio $(La/Yb)_{cn}$ in this alteration is less than that in unaltered rocks. In other words, the amount of LREEs is lower than HREEs, probably due to transport by hydrothermal solutions. In contrast, HREEs remained in the environment. The ratio $(La/Sm)_{cn}$ in this alteration zone (Fig. 6B) indicates the enrichment of MREEs compared to LREEs. This ratio decreased in altered rocks compared to unaltered ones. The correlation coefficient measured for this alteration zone (Table 7 in Appendix) shows a positive relationship between LREEs and HREEs with Al_2O_3, TiO_2, P_2O_5, Th, Ga, Hf and Zr, and a relatively positive relationship between MREEs with Zr. The results present the effect of REEs sweeping by minerals containing these elements such as clay

Table 2. Values of $(La/Yb)_{cn}$, $(La/Sm)_{cn}$, $(Tb/Yb)_{cn}$, $(Ce/Ce^*)_{cn}$, and $(Eu/Eu^*)_{cn}$ in alteration zones and unaltered rocks in exploration wells of Moyil Valley

	La/Y	$(Gd/Yb)_{cn}$	$(La/Yb)_{cn}$	$(La/Sm)_{cn}$	$(Tb/Yb)_{cn}$	$(Ce/Ce^*)_{cn}$	$(Eu/Eu^*)_{cn}$
NWS3-370	3.98	3.84	33.80	6.06	2.37	0.82	1.54
NWS1-499	6.93	5.23	53.28	6.13	2.83	0.72	0.40
NWS1-803	3.14	2.56	23.47	6.30	1.73	0.86	0.92
NWS3-692	3.32	2.77	25.65	6.17	1.90	0.83	0.87
NWS3-3082	1.52	1.92	11.14	4.21	1.48	0.85	1.62
NWS4-565	3.03	2.20	21.02	6.79	1.52	0.83	0.98
NWS4-818	3.26	2.69	24.88	6.40	1.93	0.88	1.04
NWS4-1455	3.07	2.92	24.89	5.81	2.17	0.91	0.67
NWS1-1265	3.18	2.82	24.78	5.97	1.79	0.83	1.28
NWS3-1265	4.02	2.76	30.83	7.33	1.80	0.83	0.99
NWS3-2992	1.71	1.92	12.30	4.63	1.50	0.79	1.22
NWS3-1510	2.62	2.63	20.35	5.21	1.84	0.88	0.94
NWS3-1601	2.42	2.15	18.06	5.74	1.53	0.73	0.93
NWS3-2002	2.87	3.08	23.21	5.09	2.08	0.86	0.94
NWS4-1804	2.82	2.63	21.05	5.71	2.00	0.97	0.60
NWS4-1806	2.97	2.67	21.28	5.73	2.00	0.86	0.59
NWS4-2262	1.88	2.13	13.08	4.63	1.63	0.93	1.56
NWS1-1270	3.04	2.40	22.15	6.23	1.66	0.97	0.75
NWS1-1189	3.50	2.74	26.63	6.44	1.68	1.17	0.89
NWS1- 3197	5.22	2.84	37.90	9.84	1.40	0.81	1.42
NWS1-1716	2	2.29	16.02	4.78	1.63	0.90	1.06
NWS1- 2080	2.5	2.40	18.99	5.60	1.56	0.84	0.44

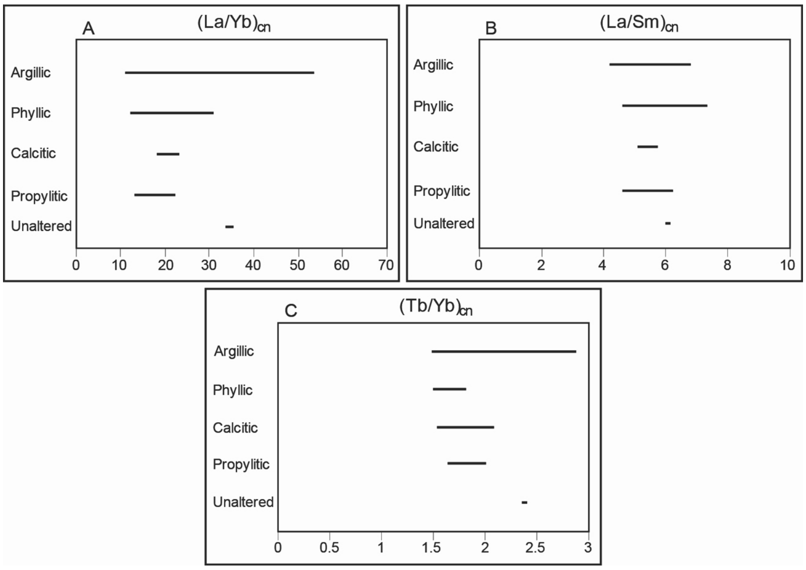

Fig. 6. Comparison of trends in changes in values of: **A –** $(La/Yb)_{cn}$; **B –** $(La/Sm)_{cn}$; **C –** $(Tb/Yb)_{cn}$ for argillic, phyllic, propylitic and calcitic alterations with trachyandesite

minerals or their presence in a mineral network of some elements such as monazite or substitution (for example, Hf and Zr in the composition of minerals). In comparison, MREEs were removed by the ligands due to a lack of correlation with the elements mentioned.

4.2.2. Phyllic alteration zone

In this zone, the mean $(La/Yb)_{cn}$, $(La/Sm)_{cn}$ and $(Tb/Yb)_{cn}$ ratios are 22.62, 5.9 and 1.69, respectively, which are lower than the equivalent values in unaltered rocks (Table 2). These ratios suggest enrichment of HREEs relative to other REEs (Fig. 6A–C). The positive and high correlation between LREEs, HREEs and MREEs with Hf, Ga and Th may be due to the presence of host minerals such as monazite (Table 7 in Appendix).

4.2.3. Propylitic alteration zone

The average $(La/Yb)_{cn}$, and $(La/Sm)_{cn}$ and $(Tb/Yb)_{cn}$ ratios in this zone are 19.39, 5.57 and 1.82, respectively. These values in equidistant unaltered rocks are 33.87, 2.37 and 6.6, respectively (Table 2). The ratio of $(La/Yb)_{cn}$ in Figure 6A indicates that LREEs and MREEs compared to HREEs are depleted during this alteration (Fig. 6B, C). Calculating the Pearson correlation coefficient for this alteration zone (Table 7 in Appendix) indicates that LREEs and MREEs have a positive and high correlation with oxides such as Fe_2O_3, TiO_2 and P_2O_5, as well as with elements such as Zr, Hf, Y and Th. The high correlation between LREEs and MREEs with Y and P_2O_5 suggests the presence of mineral enzymes in the environment. With the loss of this mineral and its depletion from the environment, REEs also entered the fluid and were depleted, while HREEs remained in the environment due to the presence of acidic fluid.

4.2.4. Calcitic alteration zone

In this alteration zone, the average $(La/Yb)_{cn}$, $(La/Sm)_{cn}$ and $(Tb/Yb)_{cn}$ ratios are lower than those in healthy rocks (Fig. 6A–C; Table 2). By calculating the Pearson correlation coefficient in this alteration zone, it appears that LREEs and HREEs have a high correlation with major rock-forming oxides such as Al_2O_3, CO_2, TiO_2 and P_2O_5 and elements such as Zr, Hf, and Y (Table 7 in Appendix).

To evaluate the fractionation degree between REEs, various ratios of REEs, such as (La/Yb)n, (La/Sm)n and (Gd/Yb)n were used. (La/Yb)n determines the degree of fractionation of LREEs from HREEs during geochemical processes (Aubert et al., 2001; Yusoff et al., 2013, Zamanian & Radmard, 2016) while the other two ratios establish the degree of fractionation between LREEs and MREEs and between MREEs and HREEs, respectively (Yusoff et al., 2013).

The values of these ratios have ranges for (La/Yb)n from 11.14 to 53.28, for (La/Sm)n from 4.21 to 9.84, and (Gd/Yb)n from 1.92 to 5.23 (Table 2). Most fractionation occurred between LREEs and HREEs (up to five times) and relatively minor fractionation between MREEs and HREE during alteration processes. These ratios reflect fractionations as follows: LREEE/HREE > LREE/MREE> MREE/HREE. The highest values of two ratios were observed in the argillic zone (La/Yb)n = 53.28 and (Gd/Yb)n = 5.23 (Table 2) that represented high fractionation of REE in ore zone, not only because of low HREE, but also because of high LREE.

Since the distribution pattern of REEs is governed by mainly geochemical conditions, the La/Y ratios provide useful information for determination of pH in the environment of ore formation. Values of La/Y > 1 show alkaline conditions, while values of La/Y < 1 indicate acidic conditions (Crinci &Jurkowic, 1990). This ratio in the Moyil Valley alteration zones ranges from 1.52 to 6.93 (Table 2). The argillic zone has the highest and lowest La/Y values (6.93–1.52). These two divisions indicate basic and very basic conditions of hydrothermal alteration that may indicate two different phases of argillic alteration in the study area.

4.3. Evolution of Eu and Ce anomalies in alteration zones

The ratios of $(Eu/Eu^*)_{cn}$ and Ce/Ce^*_{cn} were also considered for studying the behaviour of these two elements in different alteration zones. For this purpose, REEs in these samples were normalised to chondrite (Taylor &MacLennan, 1985). The Eu/Eu ratio is a measure of Eu anomaly such that if it is greater than 1, anomalies are positive and if less than 1, anomalies will be negative (Rollinson, 1993).

$$Eu / Eu^* = Eu_N / [(Sm_N) \times (Gd_N)]^{0.5} \text{ and}$$
$$Ce / Ce^* = 2Ce_N / [(La_N) + (Pr_N)]$$

where N represents the normalisation of values of elements mentioned in chondrite (Taylor & McLennan, 1985). The calculations for Eu and Ce elements for the alteration zones (Table 2) show a negative Eu anomaly for all alteration zones (Fig. 7A) in the volcanic unit. In comparison, Ce anomalies are both positive and negative in the argillic and propylitic alteration zones, negative for the anomalous

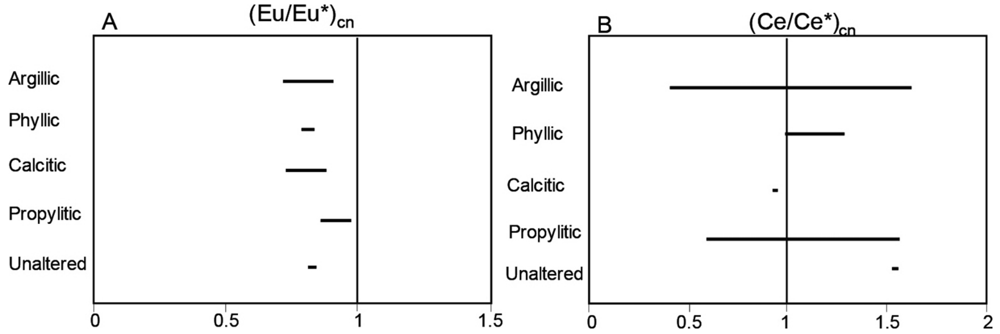

Fig. 7. Comparison of trends in changes in values of: **A –** $(Eu/Eu^*)_{cn}$; **B –** $(Ce/Ce^*)_{cn}$ for argillic, phyllic, propylitic and calcitic alterations with trachyandesite

carbonisation alteration zone and positive for the alteration zone. The calculation of this anomaly for the monzonite unit also represents a negative anomaly for Eu for the phyllic and propylitic alteration zones,,a positive anomaly of Ce for the phyllic alteration zone and a negative anomaly for the propylitic alteration zone (Fig. 7B). It seems that the main cause of the negative Eu anomaly might be the alteration of plagioclase, potassium feldspar and hornblende of the trachyandesite rock. At relatively high temperatures and in the case of a heavily reduced condition, in these minerals, Eu^{+3} leaves the system by converting to Eu^{+2} (Arslan et al., 2006). Other causes of the Eu anomaly in these alteration zones are the high activity of complex ligands, the highly acid pH of the hydrothermal solution and the increase in the fO_2 of the hydrothermal system, because Eu transfer is easy under such conditions (Sverjensky, 1984; Elderfield & Sholkovitz, 1987; Karakaya et al., 2012; Özdamar et al., 2014). However, due to very slight variations in Eu negative anomalies in the alteration zones, it can be concluded that pH changes were very small during the formation of these zones.

The negative and positive anomalies of the Ce for propylitic and argillic alteration zones may provide evidence of changing the oxidant to reduce conditions, which leads to some changes from negative to positive anomalies. Moreover, the negative Ce anomalies in the formation of calcitic alteration zones show the presence of oxidant conditions while its positive anomaly in the phyllic alteration zone may suggest predominantly reducing conditions during the development of these zones (Elderfield & Sholkovitz, 1987).

5. Conclusions

Based on the results and discussions of the present study, the following conclusions can be drawn:

- Based on XRD studies, argillic, phyllic, propylitic and calcitic alteration zones in volcanic rocks and phyllic and propylitic alteration can be detected in the monzonite unit.
- Based on the study of mass changes using the method of isocon, processes such as adsorption, sweeping and acidity conditions are three major factors in the distribution and segregation of REEs in the phyllic alteration zone. The immobility and enrichment of HREEs in comparison to other REEs can be due to adsorption by minerals such as illite, smectite and kaolinite in the argillic alteration zone, pH changes and temperature reduction in the propylitic alteration zone, pH reduction and the presence of complexing ligands CO_3^{-2} in the calcitic alteration zone.
- Study of the distribution patterns of REEs and $(La/Yb)_{cn}$, $(La/Sm)_{cn}$ and $(Tb/Yb)_{cn}$ ratios for argillic, phyllic, propylitic and calcitic alteration zones revealed that they are higher in healthy rocks compared to altered rocks, suggesting the enrichment of HREEs in comparison to LREEs and MREEs. These results could be ascribed to their sweeping by clay minerals, the presence in the mineral network of some minerals, or substitution of elements such as Hf and Zr in minerals.
- Studying the $(Eu/Eu^*)_{cn}$ and $(Ce/Ce^*)_{cn}$ ratios also suggests a negative Eu anomaly for all alterations in volcanic rocks, both positive and negative for Ce anomaly in the argillic and propylitic alteration zones, positive for phyllic alteration and negative for calcitic alteration. It seems that the negative Eu anomalies can be attributed to the alteration of plagioclase, potassium feldspar and hornblende, a high activity of complex ligands, high pH and a rise in fO_2.

Acknowledgements

The authors are grateful to the research committee of University of Tabriz for supporting this project.

References

Aghanabati, A., 2004. *Geology of Iran*. Geological Survey of Iran, Tehran, 586 pp. (in Persian).

Ahmady, I. M., Hamed., Kalioby, B. A., Aly, G. M., Tohamy, A. M. & Watanabe, K., 2015. Altered granitic rocks, Nusab El Balgum Area, Southwestern Desert, Egypt: Mineralogical and geochemical aspects of REEs. *Ore Geology Reviews* 70, 252–261.

Arslan, M., Kadir, S., Abdioglu, E. & Kolayli, H., 2006. Origin and formation of kaolin minerals in saprolite of Tertiary alkaline volcanic rocks, Eastern Pontides, NE Turkey. *Clay Minerals* 41, 597–617.

Aubert, D., Stille, P. & Probst, A., 2001. REE fractionation during granite weathering and removal by waters and suspended loads: Sr and Nd isotopic evidence. *Geochimica et Cosmochimica Acta* 64, 1827–1841.

Barrett, T.J. & MacLean, W.H., 1994. Chemostratigraphy and hydrothermal alteration in exploration for VHMS deposits in greenstones and younger volcanic rocks. [In:] Lenz, D.R. (Ed.): Alteration and Alteration Processes Associated with Ore-forming Systems. *Geological Association of Canada, Short Course Notes* 11, pp. 433–467.

Bau, M., 1991. Rare-earth element mobility during hydrothermal and metamorphic fluid-rock interaction and the significance of the oxidation state of europium. *Chemical Geology* 93, 219–230.

Bogie, I., Cartwright, A.J., Khosrawi, K., Talebi, B. & Sahabi, F. 2000. The Meshkin Shahr geothermal prospect, Iran. *Proceedings, World Geothermal Congress* 2000, 997–1002.

Crinci. J. & Jurkowic, I., 1990. Rare earth elements in Triassic bauxites of Croatia, Yugoslavia. *Travaux* 19, 239–248.

Elderfield, H. & Sholkovitz, E.R., 1987. Rare earth elements in the pore waters of reducing nearshore sediments. *Earth and Planetary Science Letters* 82, 280–288.

Emami, A., 1994. *Geological map of Meshginshahr, scale 1:100,000*. Geological Survey of Iran.

Fulignati, P., Gioncada, A. & Sbrana, A., 1999. Rare earth element (REE) behavior in the alteration facies of the active magmatic-hydrothermal system of Vulcano (Aeolian Islands, Italy). *Journal of Volcanology and Geothermal Research* 88, 325–342.

Grant, J.A., 1986. The isocon diagram – a simple solution to Gresens' equation for metasomatic alteration. *Economic. Geology* 81, 1976–1982.

Gresens, R.L., 1967. Composition-volume relationship of metasomatism. *Chemical Geology* 2, 47–55.

Hass, J.R., Shock, E.L. & Sassani, D.C., 1995. Rare earth elements in hydrothermal systems: Estimates of standard partial molal thermodynamic properties of aqueous complexes of the rare earth elements at high pressures and temperatures. *Geochimica et Cosmochimica Acta* 59, 4329–4350.

Jenner, G.A., 1996. Trace element geochemistry of igneous rocks: geochemical nomenclature and analytical geochemistry. [In:] Wyman, D.A. (Ed.): Trace element geochemistry of volcanic rocks: applications for massive sulfide exploration. *Geological Association of Canada, Short Course Notes* 12, 51–77.

Karakaya, M.C., Karakaya, N., Küpeli, S. & Yavuz, F., 2012. Mineralogy and geochemical behavior of trace elements of hydrothermal alteration types in the volcanogenic massive sulfide deposits, NE Turkey. *Ore Geology Reviews* 48, 197–224.

Leitch, C.H.B. & Lentz, D.R., 1994. The Gresens approach to mass balance constraints of alteration systems: methods, pitfalls, examples. [In:] Lenz, D.R. (Ed.): Alteration and Alteration Processes Associated with Ore-forming Systems. *Geological Association of Canada, Short Course Notes*, 11, pp. 161–192.

Lentz, D.R., 1996. Trace-element systematics of felsic volcanic rocks associated with massive sulfide deposits in the Bathurst Mining Camp: petrogenetic, tectonic and chemostratigraphic implications for VMS exploration. [In:] Wyman, D.A. (Ed.): Trace element geochemistry of volcanic rocks: applications for massive sulfide exploration. *Geological Association of Canada, Short Course Notes* 12, 359–402.

Lewis, A.J., Palmer, M.R., Sturchio, N.C. & Kemp, A.J., 1997. The rare earth element geochemistry of acid-sulfate and acid-sulfate-chloride geothermal systems from Yellowstone National Park, Wyoming, USA. *Geochimica et Cosmochimica Acta* 61, 695–706.

Lottermoser, B.G., 1990. Rare earth element and heavy metal behavior associated with the epithermal gold deposit on Lihir Island, Papua New Guinea. *Journal of Volcanology Geothermal Research* 40, 269–289.

Lottermoser, B.G., 1992. Rare earth elements and hydrothermal ore formation processes. *Ore Geology Reviews* 7, 25–41.

MacLean, W.H., 1990. Mass change calculations in altered rock series. *Mineralium Deposita* 25, 44–49.

MacLean, W.H. & Kranidiotis, P., 1987. Immobile elements as monitors of mass transfer in hydrothermal alteration: Phelps Dodge massive sulfide deposit, Matagami, Quebec. *Economic Geology* 82, 951–962.

Michard, A., 1989. Rare earth element systematics in the hydrothermal fluid. *Geochimica et Cosmochimica Acta* 53, 745–750.

Moore, C.L., 1998. Evolution of regolith development and element mobility during weathering using the isocon technique. *Geological Society of Australian Special Publications* 20, 141–147.

Özdamar, S., Ece, Ö.I., Uz, B., Boylu, F., Ercan, H.Ü. & Yanik, G., 2014. Element mobility during the formation of the Uzunisa Ordu bentonite, NE Turkey, and potential applications. *Clay Minerals*, 49, 609– 633.

Rollinson, H.R., 1993. *Using geochemical Data: Evaluvation, presentation, interpretation.* Longman Scintifiic and Technical, 352.

SKM (Sinclair Knight Merz), 2003. Mt Survey re-analysis of Sabalan project, 18 pp.

Sverjensky, D.A., 1984. Europium redox equilibria in aqueous solutions. *Earth and Planetary Science Letters* 67, 70–78.

Taylor, Y. & McLennan, S.M., 1985. *The continental crust: Its composition and evolution*. Blackwell, Oxford, 312 pp.

Terkado, Y. & Fujitani, T., 1998. Behavior of rare earth elements and other trace elements during interactions between acidic hydrothermal solutions and silicic volcanic rocks, southwestern Japan. *Geochimica et Cosmochimica Acta* 62, 1903–1917.

Yusoff, Z.M., Ngwenya, B.T. & Parsons, I., 2013. Mobility and fractionation or REE during deep weathering of geochemically contrasting granites in a tropical setting, Malaysia, *Chemical Geology* 349–350, 71–86.

Zamanian, H. & Radmard, K., 2016. Geochemistry of rare earth elements in the Baba Ali magnetite skarn deposit, western Iran – a key to determine conditions of mineralization. *Geologos* 22, 33–47.

Manuscript received: 11 May 2020
Revision accepted: 20 September 2020

Appendix

Table 3. Concentrations of major elements (wt. %) in exploratory wells in Moyil Valley.

		Sample	SiO_2	Al_2O_3	Fe_2O_3	CaO	MgO	Na_2O	K_2O	Cr_2O_3	TiO_2	MnO	P_2O_5	SrO	BaO	LOI
Trachyandesite	Fresh	S3-370	54.6	16.3	6.69	5.12	4.39	4.55	2.98	0.01	1.25	0.17	0.78	0.16	0.08	2.96
	Argillic	S1- 499	57.7	20.5	5.66	1.86	0.12	0.24	2.58	0.01	1.24	0.01	0.93	0.29	0.09	8.8
		S1- 803	60	15.45	4.98	3.43	2.07	3.41	3.48	0.01	0.87	0.09	0.41	0.08	0.09	5.58
		S3-692	59.9	15.2	5.41	3.76	1.17	4.66	1.68	0.01	0.84	0.07	0.53	0.09	0.09	6.57
		S3-3082	53.7	15.4	5.63	5.97	3.2	2.58	3.83	0.01	0.78	0.15	0.48	0.06	0.09	7.7
		S4-565	61.7	15.8	5	2.73	2.07	1.71	2.59	0.01	0.66	0.1	0.29	0.04	0.07	7.29
		S4-818	59.6	16.05	5.03	3.91	2.56	4.18	3.04	0.01	0.74	0.11	0.38	0.08	0.08	4.73
		S4-1455	53.2	15.7	6.76	6.46	3.72	4.02	2.96	0.01	1.02	0.14	0.62	0.12	0.1	3.35
	Phyllic	S1-1265	58.3	16.65	5.5	3.97	2.27	4.16	3.12	0.01	0.84	0.1	0.46	0.12	0.09	4.13
		S3-1265	61.6	16.25	4.08	3.16	1.79	4.84	3.91	0.01	0.76	0.1	0.32	0.11	0.1	2.97
		S3-2992	55.1	16.65	5.45	4.95	2.31	3.08	4.35	0.01	0.79	0.14	0.56	0.07	0.12	6.29
	Calcitic	S3-1510	53	17.8	7.39	6.1	1.66	4.72	1.94	0.01	0.87	0.16	0.75	0.1	0.1	6.05
		S3-1601	47.9	15.35	7.28	6.66	3.51	0.7	2.45	0.01	0.68	0.23	0.48	0.08	0.76	12.15
		S3-2002	51.4	17	7.27	7.39	3.05	4.39	1.26	0.01	1.02	0.14	0.78	0.16	0.06	6.74
	Propylitic	S4-1804	53.3	17.85	6.78	6.54	1.94	3.9	2.36	0.01	0.93	0.16	0.67	0.1	0.1	3.88
		S4-1806	49.8	15.15	8.16	9.16	1.5	3.02	2.1	0.01	0.8	0.1	0.57	0.11	0.03	7.52
		S4-2262	59.1	17.9	5.26	4.74	1.84	4.65	2.81	0.01	0.57	0.11	0.25	0.1	0.12	2.3
		S1-1270	52.8	18.95	6.6	4.67	3.03	6.97	0.83	0.01	0.93	0.15	0.44	0.11	0.03	4.7
Monzonite	Fresh	S1-1189	60.6	16.3	4.78	4.29	1.99	3.99	2.67	0.01	0.81	0.08	0.39	0.11	0.08	4.13
	Phyllic	S1- 3197	66.7	17.3	2.14	2.59	0.96	1.24	4.24	0.01	0.9	0.04	0.3	0.05	0.05	2.87
		S1-1716	49.4	17.95	9.19	5.9	7.45	1.96	2.38	0.02	1.18	0.13	0.59	0.07	0.14	3.59
	Propylitic	S1- 2080	53.2	19.4	6.46	4.64	2.6	4.4	4.21	0.01	0.7	0.14	0.59	0.1	0.23	3.32

Table 4. Concentrations of REEs in samples taken from Moyil Valley region based on ppm (ICP-MS)

		Sample	La	Ce	Pr	Nd	Sm	Eu	Gd	Tb	Dy	Ho	Er	Tm	Yb	Lu	ΣREE (La-Lu)
Trachyandesite	Fresh	S3-370	68.8	200	14.7	48.1	7.33	1.88	6.77	0.76	3.48	0.63	1.77	0.22	1.46	0.23	356.13
	Argillic	S1- 499	102.5	80.9	24.4	79.7	10.8	2.3	8.72	0.86	3.38	0.56	1.7	0.23	1.38	0.24	317.67
		S1- 803	48.1	79.1	9.32	30.5	4.93	1.33	4.55	0.56	2.9	0.52	1.59	0.23	1.47	0.24	185.34
		S3-692	56.5	89.2	11.15	36.7	5.91	1.52	5.29	0.66	3.22	0.6	1.73	0.26	1.58	0.24	214.56
		S3-3082	32	99.7	7.14	25.9	4.91	1.35	4.77	0.67	3.9	0.75	2.2	0.31	2.06	0.33	185.99
		S4-565	46.6	78.5	8.35	26.4	4.43	1.18	4.22	0.53	2.75	0.54	1.6	0.22	1.59	0.24	177.15
		S4-818	48.9	89	9.06	29.5	4.93	1.37	4.59	0.6	2.83	0.57	1.6	0.24	1.41	0.25	194.85
		S4-1455	59	72.2	11.7	39	6.56	1.86	6	0.81	3.63	0.74	1.97	0.3	1.7	0.3	205.77
	Phyllic	S1-1265	52.5	123	10.55	34.7	5.68	1.48	5.19	0.6	3.06	0.58	1.64	0.22	1.52	0.23	240.95
		S3-1265	56.3	95.7	10.05	31.8	4.96	1.27	4.37	0.52	2.53	0.48	1.41	0.21	1.31	0.22	211.13
		S3-2992	39.6	91.5	8.6	30.2	5.52	1.41	5.37	0.76	4.2	0.81	2.36	0.37	2.31	0.38	193.39
	Calcitic	S3-1510	64.4	113	13.57	47.4	7.98	2.19	7.23	0.92	4.61	0.87	2.48	0.37	2.27	0.36	267.65
		S3-1601	50.1	85.7	10.2	34.3	5.63	1.29	5.18	0.67	3.65	0.7	2.1	0.29	1.99	0.3	202.1
		S3-2002	74.1	136	16.85	57.6	9.4	2.51	8.52	1.05	5.01	0.91	2.54	0.36	2.29	0.34	317.48
	Propylitic	S4-1804	63.4	69.3	12.7	42.4	7.17	2.22	6.86	0.95	4.34	0.86	2.38	0.35	2.16	0.34	215.43
		S4-1806	52.5	56.7	10.56	35.9	5.92	1.64	5.71	0.78	3.57	0.71	1.9	0.29	1.77	0.3	178.25
		S4-2262	25.9	75.2	5.38	19.1	3.61	1.1	3.66	0.51	2.59	0.52	1.53	0.25	1.42	0.24	141.01
		S1-1270	59.9	80.4	11.5	38	6.21	1.87	5.62	0.71	3.76	0.7	2.06	0.31	1.94	0.34	213.32
Monzonite	Fresh	S1-1189	47.9	100	9.09	29.8	4.8	1.32	4.28	0.52	2.54	0.47	1.43	0.2	1.29	0.21	203.85
	Phyllic	S1- 3197	46.5	108	7.43	21.7	3.05	0.8	3.02	0.33	1.59	0.3	0.9	0.14	0.88	0.16	194.8
		S1-1716	44.9	90	9.58	33.6	6.07	1.71	5.56	0.77	4.15	0.78	2.33	0.34	2.01	0.32	202.12
	Propylitic	S1- 2080	55.6	43.6	10.4	35.3	6.41	1.71	6.1	0.76	4.06	0.76	2.26	0.34	2.1	0.33	169.73

Table 5. Values of Pearson correlation coefficients between REEs and main oxides in the phyllic alteration

	SiO_2	AL_2O_3	Fe_2O_3	CaO	MgO	Na_2O	K_2O	TiO_2	MnO	P_2O_5	SrO	BaO	LOI
La	0.00	−0.75	0.39	0.02	0.70	0.82	−0.79	0.79	0.35	0.41	0.97	−0.92	−0.90
Ce	−0.53	−0.38	0.83	0.54	0.95	0.39	−0.81	0.98	0.71	0.82	0.90	−0.82	−0.53
Pr	−0.36	−0.55	0.70	0.38	0.91	0.56	−0.82	0.95	0.62	0.71	0.95	−0.88	−0.68
Nd	−0.50	−0.45	0.79	0.51	0.95	0.43	−0.79	0.98	0.71	0.81	0.91	−0.82	−0.57
Sm	−0.73	−0.22	0.93	0.74	0.99	0.14	−0.68	0.98	0.84	0.94	0.75	−0.66	−0.29
Eu	−0.72	−0.20	0.94	0.73	0.98	0.15	−0.71	0.97	0.82	0.93	0.76	−0.68	−0.30
Gd	−0.85	−0.07	0.97	0.86	0.96	−0.06	−0.56	0.93	0.90	0.98	0.61	−0.50	−0.10
Tb	−0.98	0.27	0.81	0.99	0.68	−0.59	−0.01	0.57	0.90	0.88	0.03	0.10	0.46
Dy	−0.88	0.56	0.56	0.87	0.31	−0.87	0.32	0.18	0.65	0.61	−0.38	0.47	0.79
Ho	−0.81	0.62	0.46	0.80	0.18	−0.93	0.42	0.05	0.55	0.50	−0.50	0.57	0.86
Er	−0.76	0.62	0.38	0.75	0.11	−0.94	0.50	−0.03	0.50	0.44	−0.57	0.64	0.89
Tm	−0.52	0.60	0.07	0.52	−0.18	−0.95	0.74	−0.31	0.27	0.15	−0.79	0.85	0.95
Yb	−0.58	0.69	0.16	0.57	−0.14	−0.98	0.65	−0.27	0.29	0.20	−0.75	0.80	0.96
Lu	−0.52	0.60	0.07	0.52	−0.18	−0.95	0.74	−0.31	0.27	0.15	−0.79	0.85	0.95

Table 6. Values of Pearson correlation coefficients between REEs and main oxides in the argillic alteration

	SiO_2	AL_2O_3	Fe_2O_3	CaO	MgO	Na_2O	K_2O	TiO_2	MnO	P_2O_5	SrO	BaO	LOI
La	−0.05	0.89	0.32	−0.47	−0.45	−0.42	−0.41	0.82	−0.60	0.86	0.96	0.16	0.15
Ce	−0.38	−0.04	0.52	0.28	0.57	0.37	0.10	0.51	0.54	0.39	0.17	−0.29	−0.48
Pr	−0.12	0.93	0.32	−0.44	−0.46	−0.49	−0.32	0.83	−0.59	0.90	0.98	0.20	0.23
Nd	−0.17	0.93	0.34	−0.41	−0.45	−0.49	−0.30	0.84	−0.57	0.91	0.99	0.24	0.24
Sm	−0.27	0.90	0.43	−0.31	−0.38	−0.45	−0.27	0.87	−0.51	0.95	0.99	0.31	0.20
Eu	−0.45	0.78	0.63	−0.07	−0.17	−0.27	−0.22	0.92	−0.32	0.97	0.95	0.43	−0.03
Gd	−0.36	0.86	0.53	−0.21	−0.27	−0.39	−0.23	0.91	−0.40	0.98	0.98	0.31	0.11
Tb	−0.68	0.63	0.77	0.21	0.01	−0.17	−0.12	0.85	−0.12	0.93	0.83	0.57	−0.09
Dy	−0.92	0.08	0.71	0.67	0.36	0.01	0.29	0.45	0.35	0.54	0.28	0.61	−0.03
Ho	−0.89	−0.26	0.67	0.89	0.59	0.24	0.33	0.11	0.60	0.17	−0.10	0.53	−0.24
Er	−0.84	−0.18	0.52	0.77	0.44	0.04	0.42	0.07	0.49	0.17	−0.07	0.52	0.02
Tm	−0.65	−0.33	0.33	0.75	0.30	0.18	0.29	−0.18	0.35	−0.06	−0.24	0.67	−0.01
Yb	−0.52	−0.45	0.15	0.65	0.36	0.01	0.42	−0.36	0.48	−0.26	−0.46	0.28	0.18
Lu	−0.67	−0.27	0.27	0.72	0.38	−0.01	0.55	−0.22	0.43	−0.12	−0.27	0.50	0.06

Table 7. Pearson correlation coefficient results of some elements with distribution pattern of REEs in the alteration zones of exploration wells in Moyil Valley

		AL_2O_3	Fe_2O_3	CaO	MgO	K_2O	TiO_2	MnO	P_2O_5	Ga	Hf	Y	Th	Zr
Argillic	$(La/Yb)_{cn}$	0.92	0.11	−0.64	−0.8	−0.4	0.82	−0.9	0.81	0.88	0.96	−0.6	0.94	0.97
	$(La/Sm)_{cn}$	0.14	−0.4	−0.67	−0.4	−0.6	−0	−0.5	−0.2	0.44	0.47	−0.9	0.26	0.52
	$(Tb/Yb)_{cn}$	0.85	0.4	−0.34	−0.6	−0.3	0.91	−0.7	0.9	0.78	0.85	−0.3	0.82	0.88
	$(Ce/Ce^*)_{cn}$	−0.84	0.21	0.75	0.89	0.34	−0.5	0.87	−0.6	−0.7	−0.8	0.41	−0.9	−0.7
	$(Eu/Eu^*)_{cn}$	−0.63	−0.3	0.48	0.55	0.55	−0.7	0.71	−0.6	−0.8	−0.9	0.57	−0.7	−0.9
Phyllic	$(La/Yb)_{cn}$	−0.75	−0.7	−0.99	−0.8	−0.5	−0.2	−1	−1	0.81	0.75	−1	0.87	−0.2
	$(La/Sm)_{cn}$	−0.87	−0.9	−1	−0.9	−0.4	−0.4	−0.9	−1	0.67	0.87	−1	0.95	0.04
	$(Tb/Yb)_{cn}$	−0.53	−0.5	−0.9	−0.6	−0.8	0.11	−1	−0.8	0.94	0.53	−1	0.69	−0.5
	$(Ce/Ce^*)_{cn}$	−0.5	−0.5	−0.89	−0.6	−0.8	0.14	−1	−0.8	0.95	0.5	−1	0.67	−0.5
	$(Eu/Eu^*)_{cn}$	0.98	0.99	0.71	0.96	−0.4	0.89	0.32	0.81	−0	−1	0.56	−0.9	−0.7
Calcitic	$(La/Yb)_{cn}$	0.61	−0.1	0.62	−0.2	−1	0.99	−0.9	0.88	−0.1	0.7	0.94	0.31	0.91
	$(La/Sm)_{cn}$	−0.88	−0.3	−0.25	0.56	0.91	−1	0.99	−1	−0.3	−0.4	−1	−0.7	−1
	$(Tb/Yb)_{cn}$	0.71	0	0.5	−0.3	−1	1	−1	0.94	0.04	0.6	0.98	0.43	0.96
	$(Ce/Ce^*)_{cn}$	0.98	0.54	−0.05	−0.8	−0.8	0.84	−0.9	0.98	0.57	0.07	0.94	0.85	0.96
	$(Eu/Eu^*)_{cn}$	0.95	0.43	0.08	−0.7	−0.8	0.9	−1	1	0.47	0.19	0.97	0.78	0.99
Propylitic	$(La/Yb)_{cn}$	−0.12	0.78	0.42	0.33	−0.7	0.94	0.47	0.79	0.34	0.67	0.82	0.72	0.76
	$(La/Sm)_{cn}$	0.08	0.64	0.21	0.55	−0.9	0.93	0.53	0.63	0.55	0.82	0.76	0.86	0.89
	$(Tb/Yb)_{cn}$	−0.67	0.78	0.86	−0.6	0.22	0.44	0.03	0.9	−0.5	−0.2	0.57	−0.2	−0.1
	$(Ce/Ce^*)_{cn}$	0.94	−0.6	−0.78	0.71	−0.3	0.39	0.89	−0	0.76	0.63	0.46	0.56	0.58
	$(Eu/Eu^*)_{cn}$	0.3	−0.9	−0.6	−0.1	0.49	−0.9	−0.4	−0.9	−0.1	−0.5	−0.8	−0.5	−0.6